Eur. Phys. J. B **17**, 417–427 (2000)

THE EUROPEAN PHYSICAL JOURNAL B

EDP Sciences

Non-Langevin behaviour of the uncompensated magnetization in nanoparticles of artificial ferritin

C. Gilles[1], P. Bonville[1,a], K.K.W. Wong[2], and S. Mann[2]

[1] CEA, CE Saclay, Service de Physique de l'État Condensé, 91191 Gif-sur-Yvette, France
[2] School of Chemistry, University of Bristol, Bristol, UK

Received 20 January 2000

Abstract. The magnetic behaviour of nanoparticles of antiferromagnetic artificial ferritin has been investigated by ^{57}Fe Mössbauer absorption spectroscopy and magnetization measurements, in the temperature range 2.5–250 K and with magnetic fields up to 7 T. Samples containing nanoparticles with an average number of ^{57}Fe atoms ranging from 400 to 2 500 were studied. By analysing the magnetic susceptibility and zero field Mössbauer data, the anisotropy energy per unit volume is found, in agreement with some of the earlier studies, to have a value typical for ferric oxides, *i.e.* a few 10^5 ergs/cm^3. By comparing the results of the two experimental methods at higher fields, we show that, contrary to what is currently assumed, the uncompensated magnetization of the ferritin cores in the superparamagnetic regime does not follow a Langevin law. For magnetic fields below the spin-flop field, we propose an approximate law for the field and temperature variation of the uncompensated magnetization, which was early evoked by Néel but has so far never been applied to real antiferromagnetic systems. More generally, this approach should apply to randomly oriented antiferromagnetic nanoparticles systems with weak uncompensated moments.

PACS. 75.50.Tt Fine-particle systems – 75.50.Ee Antiferromagnetics – 76.80.+y Mössbauer effect; other γ-ray spectroscopy

1 Introduction

Natural ferritin is the iron-storage protein of animals, plants and bacteria. It is composed of a ferrihydrite-like core with formula $(FeOOH)_8(FeOH_2PO_4)$ about 7 nm in diameter and containing up to about 4 500 Fe atoms [1], surrounded by a 12 nm diameter multisubunit protein shell. By a suitable chemical synthesis process, it is possible to reconstitute the ferrihydrite ferritin core inside the empty protein shell (in this case obtained from horse spleen ferritin by reductive dissolution of the native core) [2]. This way, one can monitor the amount of iron available for the build up of the core, and a better control of the average core size is obtained. A number of investigations have been performed, both on natural and artificial ferritin, using either ^{57}Fe Mössbauer absorption spectroscopy [3–7] or magnetization measurements [8–11]. They have shown that the magnetic structure of the Fe^{3+} ions in the core is probably antiferromagnetic, and that the particles possess a (small) uncompensated magnetic moment. However, the interpretation of the data obtained by the two techniques is somewhat contradictory. Indeed, on one side, the Mössbauer studies with applied magnetic field [5–7] reveal that, for randomly oriented ferritin samples, the Fe^{3+} magnetic moments in the cores remain close to their easy axes, even in a strong field of 14 T. On the other side, the magnetic measurements have been interpreted so far by assuming that the uncompensated magnetization follows a Langevin law, which implicitly assumes the Fe^{3+} moments are free to rotate. Besides its fundamental interest, the understanding of the magnetic properties of ferritin is of importance for NMR relaxometry [10] and biophysical purposes as it is a good contrasting agent for NMR imaging. The ferritin core has also recently arisen great interest because it has been thought to be a good candidate for the observation of quantum tunneling of the magnetization [12], and various experimental studies, at low temperature, have claimed to have observed this tunneling [13–15].

The aim of the present work is to reexamine the problem of the uncompensated magnetization in ferritin, by comparing ^{57}Fe Mössbauer data, both in zero field and in applied fields up to 7 T, with magnetization data obtained for the same samples. We show that, by taking proper account of the crystalline anisotropy in an antiferromagnetic structure, one obtains a coherent interpretation of the results of the two techniques. We present a new interpretation of the superparamagnetic behaviour of an ensemble of randomly oriented antiferromagnetic particles, in terms of a non-Langevin law for the uncompensated

[a] e-mail: bonville@spec.saclay.cea.fr

magnetization, for applied magnetic fields lower than the spin-flop field. This approach, which was evoked by Néel in an early work [16], has however never been considered in the modern and quantitative magnetic investigations of ferritin. Another motivation of our work is to examine the influence of the mean iron content of the (artificial) ferritin core (ranging from 400 to 2 500 Fe atoms) on the physical properties, such as the anisotropy energy, or the Néel temperature.

The paper is organized as follows: Section 2 contains the description of the artificial ferritin samples, Section 3 briefly recalls the superparamagnetic behaviour of antiferromagnetic particles, both from the point of view of magnetometry and ^{57}Fe Mössbauer spectroscopy, Sections 4 and 5 contain respectively the FC-ZFC magnetic susceptibility and zero field Mössbauer measurements, and the high field Mössbauer data; in Section 6, the influence of anisotropy in uncompensated antiferromagnets is examined, and Section 7 reports the magnetization experiments and the new interpretation we propose.

2 Sample characterization and experimental techniques

In order to investigate the effect of decreasing both the particle size and the mean number of Fe atoms per ferritin core, the experiments were performed with a set of artificial ferritin samples with different Fe loadings. Five samples were studied, having an average iron loading ranging from 400 to 2 500 Fe ions per ferritin core. In order to obtain a good signal to noise ratio in the Mössbauer spectra, the Mohr salt used as the starting material was prepared with iron 95% enriched in ^{57}Fe. The protein concentration was determined by the Lowry method and the mean iron content by atomic adsorption analysis. In the following, the samples will be labelled according to the mean number of Fe atoms per core determined by this latter method. The samples consist of a solution of artificial ferritin with a concentration of about 10 mg/ml, that is ten times smaller than the concentration of commercial ferritin (about 100 mg/ml). Then, the distance between particles in the solution is about 50 nm, which corresponds to a dipolar field of magnitude 10 mG (at saturation of the uncompensated moments). Our samples can therefore be considered as an ensemble of non-interacting particles. Pictures taken by transmission electron microscopy (TEM) show the cores to be discrete and roughly spherical in shape. Size histograms have been established by measuring the diameter of 500 particles taken from different parts of the grid. For each sample, the diameter distribution is rather narrow and can be fitted to a lognormal shape, with a mean diameter d_0 ranging from 4 nm for the particles with 400 Fe atoms per core to 5.7 nm for the particles with 2 571 Fe atoms per core, and a standard diameter deviation σ about 0.15. Electron diffraction patterns, performed on the particles with 2 571 Fe atoms per core, give d-spacings corresponding to well-ordered ferrihydrite.

The magnetization measurements were made with a commercial SQUID magnetometer in magnetic fields up to 5.5 T in the temperature range 2.5–250 K. For all temperatures and fields, we have measured both the signal of the solution containing ferritin and the signal of the solution containing apoferritin (the empty protein shells) with the same concentration. After subtraction of the second signal from the first, we thus obtain the signal due only to the ferritin cores. For the low field (80 G) magnetization measurements, both Field Cooled (FC) and Zero Field Cooled (ZFC) branches were measured. In the Zero Field Cooled (ZFC) procedure, the sample was cooled in zero field from room temperature down to 2.5 K, and for the Field Cooled (FC) branch, the sample was cooled with a field of 80 G from room temperature to 2.5 K; in both cases, measurements proceeded on heating.

The ^{57}Fe Mössbauer absorption spectroscopy experiments were performed both in zero magnetic field and in magnetic fields up to 7 T applied perpendicular to the γ-ray propagation direction, between 4.2 K and 90 K. The Mössbauer spectra were obtained using a ^{57}Co:Rh source, mounted on an electromagnetic drive with a triangular velocity signal. The ferritin solution was placed in a copper holder covered with pure thin aluminium sheets, ensuring a good thermalization. For the in-field measurements, the ferritin solution is first frozen in zero field and therefore there is no preferential orientation of the magnetization of the particles.

3 Superparamagnetism of antiferromagnetic particles

The Fe^{3+} ion has a saturated magnetic moment $m_0 = 5\ \mu_B$. The magnetic structure of the ferritin cores is expected to be antiferromagnetic, with a Néel temperature T_N of the order of a few hundred Kelvins. In zero external field, the preferential orientation of the two antiferromagnetic sublattices in the core is determined by the crystalline anisotropy ("antiferromagnetic axis"). For antiferromagnetic nanometric particles, one expects a small uncompensated magnetization which may arise from the core (presence of defects) and/or from the unpaired surface moments of the particle [17]. Due to the strong exchange interaction, the uncompensated moments are aligned with the antiferromagnetic sublattice moments, except probably at the surface due to broken exchange bonds [18]. At a given temperature T below T_N, the moments of the two sublattices fluctuate by crossing the anisotropy energy barrier: this is the superparamagnetic relaxation. In the case of an axial anisotropy, the relaxation time for the reversal of the direction of the magnetization of a particle with volume V is described by an Arrhenius type equation first proposed by Néel [19]:

$$\tau = \tau_0 \exp\left(\frac{KV}{k_B T}\right), \quad (1)$$

where K is the magnetic anisotropy energy per unit volume, τ_0 a microscopic relaxation time usually considered

to be a constant with magnitude 10^{-10}–10^{-11} s but varying in fact with V and T [20]. Due to the particle size distribution present in any real sample, there is a distribution of anisotropy barriers KV which, according to equation (1), results in a broad distribution of relaxation times. For a given measurement technique, with a characteristic time $\tau_{\rm m}$, the blocking volume:

$$V_{\rm b} = \frac{k_{\rm B}T}{K} \ln(\tau_{\rm m}/\tau_0), \tag{2}$$

defines two populations of particles: those with $V > V_{\rm b}$ and those with $V < V_{\rm b}$, whose magnetization fluctuation time is respectively larger and smaller than $\tau_{\rm m}$. Using equation (1), one can also define a mean blocking temperature:

$$T_{\rm b} = \frac{K\langle V\rangle}{k_{\rm B} \ln(\tau_{\rm m}/\tau_0)}, \tag{3}$$

such that, for $T \ll T_{\rm b}$ all the particles are in the "frozen regime" and for $T \gg T_{\rm b}$ all the particles are in the "superparamagnetic regime".

For magnetization experiments, the characteristic time can be considered to be the measurement time τ_χ, which is about 100 s. In low fields, and for the superparamagnetic regime, Néel has shown that the magnetization is the sum of two contributions [21]:

$$M(H,T) = \chi_{\rm AF} H + M_{\rm nc}(H,T), \tag{4}$$

where $\chi_{\rm AF}$ is the susceptibility arising from the canting of the two antiferromagnetic sublattices, and $M_{\rm nc}$ is the magnetization due to the uncompensated moments. At $T = 0$ and in the case the magnetic field is perpendicular to the antiferromagnetic axis, $\chi_{\rm AF} = \chi_\perp$ which, in the standard molecular field theory, is given by: $\chi_\perp = M_0/H_{\rm E}$, M_0 being the magnetization of a sublattice and $H_{\rm E}$ the exchange field. In the low field limit, the uncompensated magnetization follows a Curie law, irrespective of the strentgh of the anisotropy [21]. At higher fields, the choice of an expression for $M_{\rm nc}(H,T)$ is not a trivial problem, and an important issue of the present work is the determination of the best approximation for the field and temperature dependence of the uncompensated magnetization in antiferromagnetic particles.

The characteristic Mössbauer time is the Larmor period $\tau_{\rm L}$ associated with the magnetic hyperfine interaction. For ^{57}Fe, it is of the order of 5×10^{-9} s. In the case of magnetic ordering of the Fe^{3+} ions, there is a magnetic hyperfine field $\mathbf{H}_{\rm hf}$ at the nucleus, proportional to the Fe^{3+} moment and directed opposite to it. If the fluctuation time τ of the magnetization (and hence of the hyperfine field) is longer than $\tau_{\rm L}$, the Mössbauer spectrum is a six-line hyperfine field pattern; if it is smaller than $\tau_{\rm L}$, the Mössbauer spectrum is a two-line quadrupolar pattern. In real systems, due to the broad distribution of τ values, a zero field pattern consists of a superposition of magnetic and quadrupolar subspectra, in a sizeable temperature range. When a magnetic field is applied, each nucleus

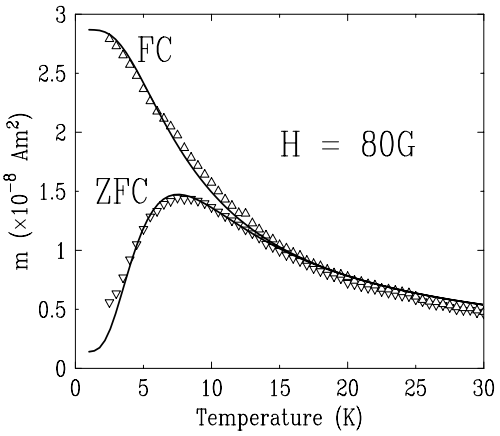

Fig. 1. Thermal variation of the FC and ZFC magnetic susceptibility in the artificial ferritin sample with a mean Fe loading of 410 atoms per core, measured in a field of 80 G. The solid lines are fits using to equation (7) and a Gaussian distribution of $\mu_{\rm nc}$ values.

experiences an effective field $\mathbf{H}_{\rm eff}$, which is the vectorial sum of the applied field $\mathbf{H}$ and of the hyperfine field $\mathbf{H}_{\rm hf}$:

$$\mathbf{H}_{\rm eff} = \mathbf{H} + \mathbf{H}_{\rm hf}. \tag{5}$$

If ϕ is the angle between the γ-ray propagation direction and the effective field direction, the intensity ratios of the outer to middle to inner pairs of lines of the Mössbauer sextet are given by:

$$3(1 + \cos^2\phi) : 4\sin^2\phi : (1 + \cos^2\phi). \tag{6}$$

If the effective field is aligned perpendicular to the γ-ray direction, the intensity ratios are 3:4:1, and for a random orientation of the effective field, the intensity ratios are 3:2:1.

4 Low field susceptibility and zero field Mössbauer experiments

The two FC and ZFC branches of the magnetic susceptibility for the particles with 410 Fe atoms per core, measured in a field H=80 G, are represented in Figure 1. The signal is almost entirely due to the uncompensated moments, the antiferromagnetic susceptibility being very weak as will be shown in Section 7.

The shape of the curves is typical of an ensemble of non-interacting relaxing moments with a distribution of anisotropy barriers [22]. The peak temperature of the ZFC curve for the particles with 410 Fe atoms per core is $T_{\rm peak} \simeq 7.5$ K, and the irreversibility temperature at which the FC and ZFC branches join is $T_{\rm irr} \simeq 15$ K. To interpret these curves, we follow here the model of reference [22]. Assuming that, for a given particle volume, the uncompensated moment $\mu_{\rm nc}$ is a known function of V, the thermal variation of the FC and ZFC magnetic

moment writes:

$$m_{\rm nc}(T) = \frac{H}{3k_{\rm B}T}\int_{V_{\rm min}}^{V_{\rm b}(T)} \mu_{\rm nc}(V)^2 f(V){\rm d}V + \eta\frac{H}{3K}\int_{V_{\rm b}(T)}^{V_{\rm max}} \mu_{\rm nc}(V)^2\frac{f(V)}{V}{\rm d}V, \qquad (7)$$

where $f(V)$ is the log-normal volume distribution function, $V_{\rm b}(T)$ the blocking volume associated with τ_χ, and with $\tau_0 = 10^{-11}$ s, and η=0 for the ZFC branch and $\ln\frac{\tau_\chi}{\tau_0}$ for the FC branch. However, in antiferromagnetic particles, the relationship between volume and uncompensated moment is not well known. The most probable is that, for a given volume, there is a distribution of uncompensated moment values. According to an argument due to Néel [17], the mean value of this distribution is proportional to N^p, where N is the number of Fe atoms in the particle and $p = 1/2$, $1/3$ or $2/3$ in the case respectively of a random distribution of the uncompensated moments in the volume, at the surface, or in the presence of regular "active" (ferromagnetic) planes at the surface. It appears that the fit of the experimental FC and ZFC curves using equation (7) is not very sensitive to the particular shape of the distribution of uncompensated moments, nor to the choice of a particular p value. The solid lines in Figure 1, which reproduce quite well the experimental data, were obtained by introducing a Gaussian distribution of $\mu_{\rm nc}$ values into expression (7).

The mean value of this distribution is taken as: $\langle\mu_{\rm nc}\rangle = m_0 u\sqrt{N}$ (assuming the Fe atomic density $n = N/V$ is constant for a given particle set), and its standard deviation as $\sigma_{\rm nc} = 0.4\langle\mu_{\rm nc}\rangle$. The distribution is restricted to positive $\mu_{\rm nc}$ values. The fitted value of the proportionality parameter u is in the range 0.8–1 for the different particle sets, and the standard deviation of the diameter distribution was kept at the value $\sigma = 0.15$ obtained from the size histograms. This choice of a $N^{\frac{1}{2}}$ law for the mean $\mu_{\rm nc}$ value corresponds to a volumic random distribution of the Fe atoms bearing the uncompensated moments but, as emphasized before, the data do not allow us to exclude the presence of uncompensated moments at the surface. Nevertheless, these fits allow the anisotropy constant K to be determined: we find that K lies in the range 3–6×10^5 ergs/cm^3 for the different particle sets, with a tendency to increase as the particle size decreases.

In Figure 2 is represented, for each sample, the behaviour of the ZFC magnetization as a function of temperature (the fit is shown as a solid line only for the particles with 2 571 Fe atoms per core). The peak temperature increases with the particle size, and it varies approximately linearly with the mean barrier energy $K\langle V\rangle$, as can be seen in Figure 3. As, in antiferromagnetic particles, the shape anisotropy is very small [23], this linear correlation is expected if the volumic anisotropy dominates over the surface anisotropy. Indeed, in this case, $T_{\rm peak}$ can be shown to be proportional to the blocking temperature $T_{\rm b}$ [22,24]:

$$T_{\rm peak} = g(\sigma)T_{\rm b}, \qquad (8)$$

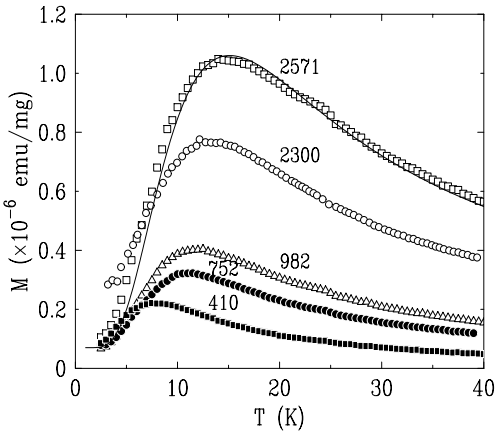

Fig. 2. Thermal variation of the magnetization of artificial ferritin samples with different Fe loadings (the figure near each curve represents the mean number of Fe atoms per particle) upon warming in a field of 80 G after cooling in zero field (ZFC curves). The fit using equation (7) (solid lines) is shown only for the sample with a loading of 2 571 Fe atoms per core. The magnetization is expressed in emu per mg of protein.

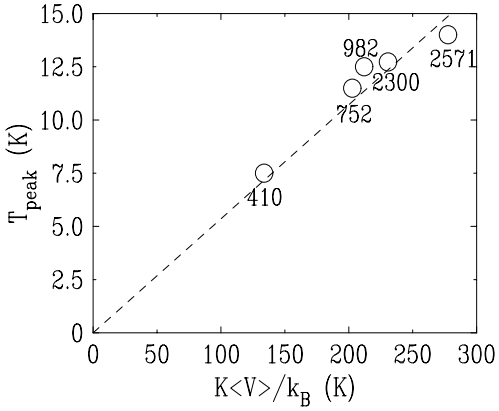

Fig. 3. Dependence of $T_{\rm peak}$ of the ZFC curves on the mean anisotropy energy in artificial ferritin samples.

where $g(\sigma)$ is an increasing function of the standard diameter deviation σ with $g(\sigma\to0) = 1$. As σ is relatively constant for the different particle sets, the peak temperature must be proportional to the mean anisotropy barrier owing to equation (3).

For all samples, the FC curve joins the ZFC curve above an irreversibility temperature which is about twice the peak temperature; therefore, for all particle sizes, the superparamagnetic regime associated with the magnetization measurement time occurs above 30 K.

Representative ^{57}Fe Mössbauer absorption spectra in zero field for the particles with 410 Fe atoms per core are shown in Figure 4. At 4.2 K, a static magnetic hyperfine pattern is observed with a hyperfine field $H_{\rm hf} \simeq 490$ kOe, identical for all particle sets. As temperature increases, the quadrupolar doublet progressively replaces the six-line magnetic pattern as the superparamagnetic fluctuation time of more and more particles becomes smaller than $\tau_{\rm L}$, *i.e.* as the blocking volume given

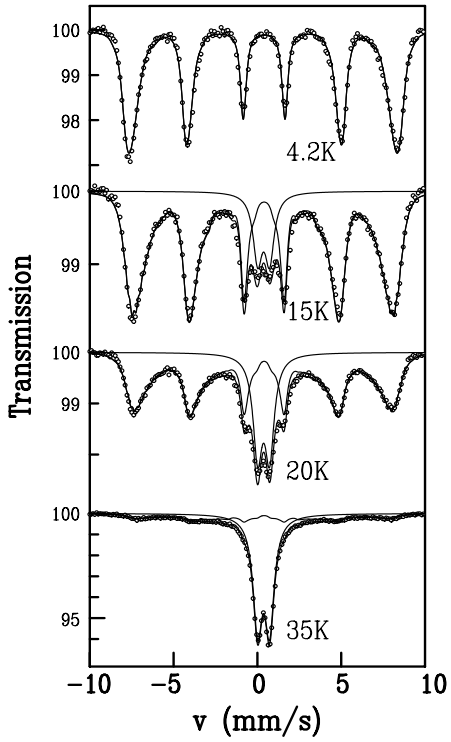

Fig. 4. ^{57}Fe Mössbauer absorption spectra at selected temperatures in zero field in the artificial ferritin sample with a mean Fe loading of 410 atoms per core.

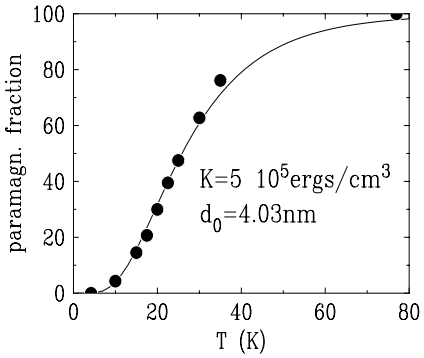

Fig. 5. Thermal variation of the relative intensity of the quadrupolar doublet in the artificial ferritin sample with a mean Fe loading of 410 atoms per core. The solid line is a fit using equation (9). The blocking temperature is 22 K.

by equation (2) associated with the characteristic time $\tau_{\rm L}$ becomes smaller. The spectra were fitted to a superposition of a quadrupolar hyperfine spectrum and of magnetic hyperfine spectra with a distribution of hyperfine fields (histogram).

The thermal variation of the relative intensity $f_{\rm p}(T)$ of the quadrupolar doublet derived from these fits is shown in Figure 5. This "paramagnetic fraction" can be calculated in the frame of Néel's model of thermally activated fluctuations:

$$f_{\rm p}(T) = \frac{1}{\langle V \rangle} \int_{V_{\rm min}}^{V_{\rm b}(T)} V f(V) {\rm d}V, \qquad (9)$$

where $V_{\rm b}(T) = \frac{k_{\rm B}T}{K} \ln \frac{\tau_{\rm L}}{\tau_0}$ and $\tau_0 = 10^{-11}$ s. The paramagnetic fraction is independent of the values (or distribution) of the uncompensated moments as long as one neglects the possible (but unknown in antiferromagnets) dependence of τ_0 on $\mu_{\rm nc}$. For all particle sets, the thermal variation of $f_{\rm p}$ is well reproduced using equation (9) (solid line in Fig. 5), with an anisotropy constant close to that derived from the fit of the FC-ZFC susceptibility curves. The blocking temperature, defined as the temperature for which half of the particles are in the superparamagnetic regime, increases with the particle mean size. For all iron loadings, all the particles are in the superparamagnetic regime above 80–100 K.

5 High-field Mössbauer experiments

According to the zero field Mössbauer data, for all particle sizes, the fluctuations of the magnetization at 4.2 K are slow with respect to the hyperfine Larmor frequency, and they are fast at 90 K. In-field Mössbauer spectra at these temperatures have been recorded in natural ferritin and haemosiderin in reference [5]. We repeated these measurements in our artificial ferritin samples to try and detect the influence of the particle size on the orientation of the magnetic moments in the frozen and paramagnetic regimes when a magnetic field up to 7 T is applied. We actually found that there is no drastic qualitative change of the in-field spectra for the different particle sets, and our data are similar to those recorded in natural ferritin. We therefore only present the spectra for the particles with 410 Fe atoms per core, and our interpretation follows the same lines as that made in reference [5].

5.1 Spectra in the frozen regime (T = 4.2 K)

The spectra at 4.2 K for fields of 3 T and 7 T in these particles are shown in Figure 6. They are resolved six line hyperfine spectra, analogous to the zero-field spectrum (see top of Fig. 4). The intensity ratios of the pairs of lines remain close to 3:2:1, even at 7 T, which means that the field does not drastically modify the orientations of the individual Fe^{3+} moments with respect to those in the randomly oriented zero-field configuration. The spectra were then fitted assuming random orientations of the static hyperfine field $\mathbf{H}_{\rm hf}$, with fixed magnitude. For a given angle $\theta_{\rm b}$ between $\mathbf{H}_{\rm hf}$ and the applied field, the magnitude of the effective field $\mathbf{H}_{\rm eff} = \mathbf{H} + \mathbf{H}_{\rm hf}$ experienced by the nucleus is given by:

$$H_{\rm eff} = \{(H_{\rm hf} \cos\theta_{\rm b} + H)^2 + H_{\rm hf}^2 \sin^2\theta_{\rm b}\}^{\frac{1}{2}}. \qquad (10)$$

The orientational disorder of $\mathbf{H}_{\rm hf}$ yields then a small distribution of the magnitude of $H_{\rm eff}$. It entirely accounts

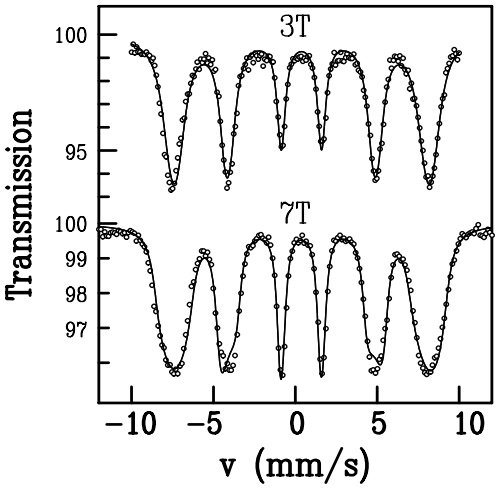

Fig. 6. ^{57}Fe Mössbauer absorption spectra in the frozen regime (4.2 K) in the artificial ferritin sample with a mean Fe loading of 410 atoms per core, with magnetic fields of 3 T and 7 T applied perpendicular to the γ-rays propagation direction. The solid lines are a fit to a model with random orientation of the hyperfine fields.

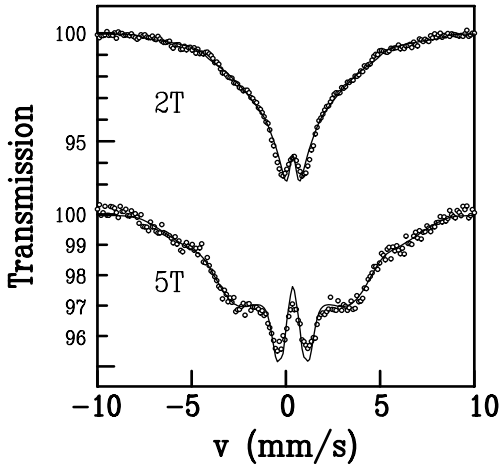

Fig. 7. ^{57}Fe Mössbauer absorption spectra in the superparamagnetic regime (T = 90 K), in the artificial ferritin sample with a mean Fe loading of 410 atoms per core, with magnetic fields of 2 T and 5 T applied perpendicular to the γ-rays propagation direction. The solid lines correspond to fits using the dynamic "random magnetic orientation" model (see text).

for the broadening of the lines with respect to the zero-field linewidths, which is the most visible at 7 T.

As seen in Figure 6, the model of a random orientation of the moments satisfactorily reproduces the shape of the Mössbauer spectra, except for a small misfit of the shape of the intermediate pair of lines. This implies that, up to a field of 7 T, the magnetic moments of the Fe^{3+} ions remain close to the antiferromagnetic axis in our ferritin samples at 4.2 K. The same qualitative conclusion can be drawn from the 14 T spectrum in horse spleen ferritin of reference [7]. In the following, we will label this moment configuration as the "random magnetic orientation" configuration.

5.2 Spectra in the superparamagnetic regime (T = 90 K)

In the superparamagnetic regime and in zero applied field, the fast fluctuations of the hyperfine field smear out the magnetic hyperfine structure. At 90 K, the zero field spectrum is a quadrupolar doublet identical with the main component of the spectrum at 35 K shown at the bottom of Figure 4. If a field is applied, the shape of the spectra, shown in Figure 7, changes, and at 5 T a six line hyperfine field pattern is distinguishable, but with large broadenings. In order to interpret the spectra, we will assume that a dynamic "random magnetic orientation" model holds at 90 K, *i.e.* that the moments fluctuate along or close to the antiferromagnetic axis. Our analysis follows here that of reference [5]. For a given orientation θ_b of the antiferromagnetic axis and a given value of the uncompensated moment, the energies of the two particle states with "up" and "down" orientations of the uncompensated moment are separated by a Zeeman splitting:

$$\Delta E_z = 2\mu_{nc}(V)H\cos\theta_b. \quad (11)$$

At a given Fe site, the hyperfine fields associated with each energy level are opposite, resulting in a thermally averaged hyperfine field:

$$H_{hf}(T,V) = H^0_{hf}(T)\tanh\left[\frac{\mu_{nc}(V)H\cos\theta_b}{k_BT}\right], \quad (12)$$

where $H^0_{hf}(T)$ is the local hyperfine field. The values of $H_{hf}(T,V)$ for a given particle set are therefore distributed due to both the distribution of $\mu_{nc}(V)$ values and to the random distribution in θ_b values.

The fits of the in-field spectra with this dynamic "random magnetic orientation" model, like those of the FC-ZFC curves, are rather insensitive to both the assumption made about the distribution of uncompensated moment values and the value of the exponent p. For the fits shown as solid lines in Figure 7, we used the same distribution of uncompensated moments as for the fits of the FC-ZFC curves, *i.e.* a truncated Gaussian shape with a mean value: $\langle\mu_{nc}\rangle = m_0 u\sqrt{N}$. We find that the parameter u is 0.4–0.5 for the lowest fields, and that it decreases as the field increases. The good reproduction of the spectral shape, especially if one considers that u is the only adjustable parameter, indicates that it is realistic to consider that the individual moments, and hence the sublattice magnetizations, fluctuate along or close to the antiferromagnetic axis at 90 K. The fact that the mean uncompensated moment found here is about twice smaller than that derived from the FC-ZFC curves probably originates from the roughness of the assumption of a Gaussian distribution of μ_{nc} values. The decrease of u as the field increases, also observed in reference [5], is probably due to the fact that the "random magnetic orientation" model starts to break down at the higher fields, as will be discussed in the next section. The values obtained for u at the lowest fields ($\sim$0.5) are similar to those derived from the magnetization measurements described in Section 7.

6 Interplay of the exchange, Zeeman and anisotropy energies in uncompensated antiferromagnets

Before proceeding with the experimental results of the magnetization measurements and their interpretation, we will examine the effect of a magnetic field on an uncompensated antiferromagnetic particle, and determine the field range for which the "random magnetic orientation" configuration is expected to be a correct approximation. For a fully compensated antiferromagnet, the relevant threshold field is the so-called spin-flop field which writes: $H_{\rm sf} \simeq \sqrt{2H_{\rm A}H_{\rm E}}$, where $H_{\rm E}$ is the exchange field and $H_{\rm A} = \frac{K}{M_0}$ the anisotropy field, M_0 being the magnetization of one sublattice [25]. When the applied field **H** is aligned along the antiferromagnetic axis, the sublattice magnetic moments rotate to a direction perpendicular to it for $H = H_{\rm sf}$. For a particular orientation $\theta_{\rm b}$ of the antiferromagnetic axis with respect to **H**, the $T = 0$ equilibrium direction θ of the sublattice moments, in the limit $H/H_{\rm E} \ll 1$ and $H_{\rm A}/H_{\rm E} \ll 1$, is given by [26]:

$$\cos^2\theta = \frac{1}{2} + \frac{\cos^2\theta_{\rm b} - \frac{1+x^2}{2}}{\sqrt{(1+x^2)^2 - 4x^2\cos^2\theta_{\rm b}}}, \qquad (13)$$

where $x = H/H_{\rm sf}$. For all initial orientations, a crossover to a "quasi spin-flop" configuration, where the equilibrium orientations are close to 90°, occurs for $H > H_{\rm sf}$ and, for lower fields, the equilibrium position θ remains close to the initial orientation $\theta_{\rm b}$.

In order to investigate the effect of the uncompensated moment, we will follow a model developed by Mørup [27]. For a particle with volume V and "degree of uncompensation" $\alpha = \mu_{\rm nc}/M_0V$, the energy of an antiferromagnetic particle is given by:

$$E(\theta,\theta_{\rm b}) = M_0H_{\rm E}[-(1+\alpha) + \frac{1}{2}\beta^2\sin^2\theta + \alpha\beta\cos\theta + \kappa(1+\alpha)\cos^2(\theta-\theta_{\rm b})], \qquad (14)$$

where $\beta = H/H_{\rm E}$ and $\kappa = H_{\rm A}/H_{\rm E}$. This expression is valid for $\beta \ll 1$, $\kappa \ll 1$ and when the "canting angle" 2ϵ of the two sublattices has its equilibrium (small) value: $2\epsilon = \beta\sin\theta$. Mørup has shown that the spin-flop field in the presence of an uncompensated moment is enhanced with respect to $H_{\rm sf}$ [27]:

$$H_{\rm sf}^{\rm nc} = \frac{1}{2}\alpha H_{\rm E} + \sqrt{\frac{1}{4}\alpha^2H_{\rm E}^2 + H_{\rm sf}^2}\,. \qquad (15)$$

In our ferritin samples, using for instance the values for the sample with 410 Fe atoms per core: $K \simeq 5\times10^5$ ergs/cm^3 and the atomic density: $N \simeq 1.2\times10^{22}$ Fe^{3+}/cm^3, the anisotropy field is: $H_{\rm A} \simeq 0.18$ T. The exchange field is more difficult to estimate because various values for $T_{\rm N}$ have been given in the literature. We will take here our estimation of the Néel temperature, which we show is close to 500 K for all particle sizes (see Sect. 7). Using the simple molecular field result: $k_{\rm B}T_{\rm N} = \frac{1}{3}g(S+1)H_{\rm E}\mu_{\rm B}$, one obtains an exchange field $H_{\rm E} \simeq 320$ T. As to the values of the degree of uncompensation α, they are probably distributed within a given particle set; using as a reasonable estimate of the mean uncompensated moment: $\langle\mu_{\rm nc}\rangle = 0.5m_0\sqrt{N}$, we find that the mean value of α ranges from 2% for the biggest particles to 5% for the smallest ones.

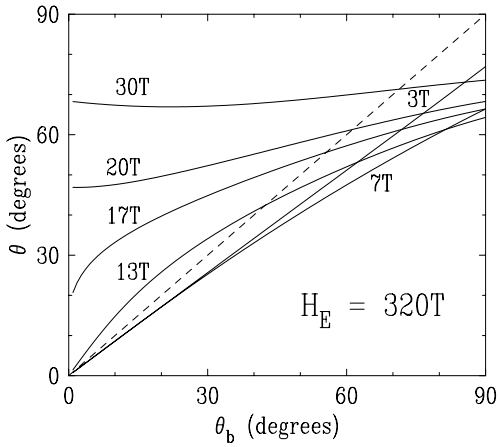

Fig. 8. Variation of the equilibrium orientation θ of the sublattice magnetizations in an uncompensated antiferromagnet as a function of the orientation $\theta_{\rm b}$ of the antiferromagnetic axis with respect to the applied field, for $H_{\rm E} = 320$ T. The ratio of the uncompensated moment to the sublattice magnetic moment is: $\alpha = 0.03$. The curves (solid lines) are calculated for different values of the applied field H ranging from 3 T to 30 T. The dashed line is the curve $\theta = \theta_{\rm b}$.

In Figure 8, we show the curves giving the $T = 0$ equilibrium orientations θ as a function of the initial orientation $\theta_{\rm b}$, for the representative value $\alpha = 0.03$, and for different values of the applied field H. For this α value, the spin-flop field is: $H_{\rm sf}^{\rm nc} = 16.6$ T. For fields below 7 T, Figure 8 shows that the equilibrium orientation θ does not strongly depart from $\theta_{\rm b}$ for all initial orientations. Thus the $T = 0$ "random magnetic orientation" model is seen to be a good approximation for fields lower than the maximum field of our experiments (7 T), thus justifying the use of this approximation to account for the $T = 4.2$ K in-field Mössbauer spectra. This model starts to break down for a field around 7 T and, above the spin-flop field, the equilibrium θ value is seen to be quasi independent of $\theta_{\rm b}$ and growing towards 90° as the field is further increased.

For a fully compensated antiferromagnetic particle, the energy profiles present two equally deep potential wells, separated by π, corresponding to the invariance of the system by inversion of the two sublattice moments. When the particle possesses an uncompensated moment, this symmetry is broken and the energy profiles become asymmetrical, as shown in Figure 9 which represents $E(\theta,\theta_{\rm b} = 50°)$ from equation (14) for different applied fields up to 15 T, and for $\alpha = 0.03$, $H_{\rm E} = 320$ T and $H_{\rm A} = 0.18$ T. The two potential wells are still clearly present for fields below 5 T, the energy difference between the lowest points in each well being essentially the Zeeman splitting given by equation (11). At higher fields (7–10 T), the less shallow

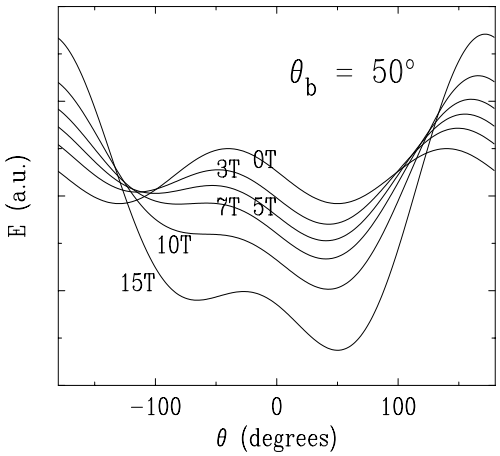

Fig. 9. Energy profile for an uncompensated antiferromagnet, for $\theta_b = 50°$, a degree of uncompensation $\alpha = 0.03$ and an exchange field $H_E = 320$ T, for different values of the applied field. The other parameters correspond to the particles with 410 Fe atoms per core.

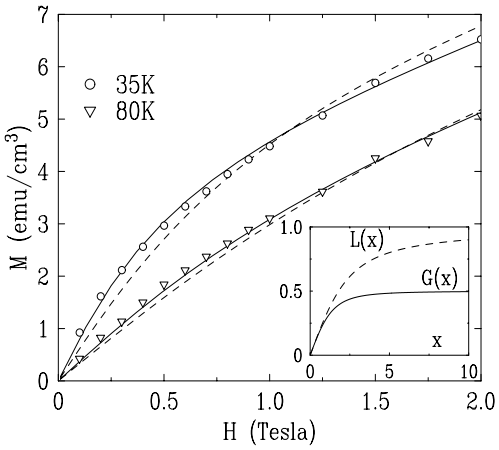

Fig. 10. Low field part of the isothermal magnetization at 35 K and 80 K in the artificial ferritin sample with a mean Fe loading of 982 atoms per core. The solid lines are fits with the "random magnetic orientation" model (see text), and the dashed lines represent the fits with the Langevin model. The inset shows the $G(x)$ function (see text) and the Langevin function $L(x)$.

well is somehow smeared out and it appears anew when the field is further increased.

The field range where only one potential well is present is such that the Zeeman energy associated with the uncompensated moment $\mu_{nc}H$ is larger than the anisotropy energy KV, but smaller than the Zeeman energy associated with the canting of the two antiferromagnetic sublattices, $\chi_\perp H^2$. When α is not too small, this yields the approximate boundaries: $H_A/\alpha < H < \alpha H_E$, *i.e.* this region lies between 6 and 9.6 T for $\alpha = 0.03$. At low fields ($H < H_A/\alpha$), the positions of the two wells remain close to θ_b for the shallowest (see Fig. 8) and $\pi - \theta_b$ for the other. Therefore, in this field region and in the superparamagnetic regime, the dynamic "random magnetic orientation" model, where the uncompensated moment is taken to fluctuate along the antiferromagnetic axis, is a fairly good approximation. At higher fields, the positions and shape of the potential wells start to be strongly modified, which probably accounts for the difficulty of coherently reproducing the Mössbauer spectra at 90 K using this model.

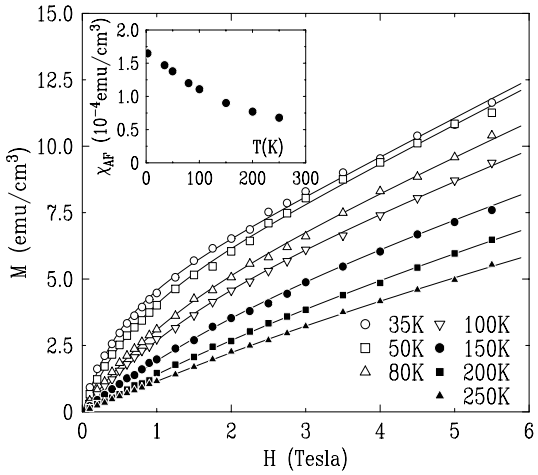

Fig. 11. Magnetization curves in the artificial ferritin sample with a mean Fe loading of 982 atoms per core. The solid lines are obtained by using the "random magnetic orientation" model (see text, Eq. (18)) The inset shows the thermal variation of χ_{AF} in the same sample.

7 Isothermal magnetization experiments

Isothermal magnetization measurements have been performed in the superparamagnetic regime, between 35 K and 250 K, for fields up to 5.5 T. Representative curves are shown in Figures 10 and 11, for the particles with 982 Fe atoms per core. For a given temperature, the magnetization increases with the field, without saturating, and, for a given field, it decreases with increasing temperature, as observed in references [8–11].

For these antiferromagnetic particles, the magnetization can be thought to arise from two contributions, as explained in Section 3: a linear term $\chi_{AF}H$, where χ_{AF} is the powder antiferromagnetic susceptibility and accounts for the weak canting of the two sublattices, and another term due to the uncompensated moments. In the previous magnetization studies of ferritin quoted above, this latter contribution has been interpreted using the Langevin model. However, for such low fields, the discussion presented in Section 6 shows that the uncompensated moments must be considered as fluctuating essentially along the antiferromagnetic axis, which is confirmed by the analysis of the in-field Mössbauer spectra at 90 K. This is not compatible with the Langevin model, which assumes the moments are free to rotate. In this respect, weakly uncompensated antiferromagnetic particles strongly differ from ferro- or ferrimagnetic particles. In the latter, the anisotropy energy is easily overcome by the Zeeman energy and the Langevin model is a good approximation, although deviations from it have been observed at low temperature

and interpreted using a full Boltzmann calculation of the magnetization (see for instance Ref. [28]). In randomly oriented antiferromagnetic particles, a calculation of the total magnetization along the same lines is much more difficult because it involves four variables, *i.e.* two positional angles for the each of the two sublattices. Therefore, as a low field approximation, we interpret the contribution of the uncompensated moments in the superparamagnetic regime using the dynamic "random magnetic orientations" model, assuming that they fluctuate between two antiparallel directions along the antiferromagnetic axes. The uncompensated moment, for a given particle volume and a given orientation, is then described by a hyperbolic tangent function similar to the expression for the hyperfine field (Eq. (12)), and the measured moment is obtained by integration over the random directions of the antiferromagnetic axis:

$$m_{\rm nc}(T,V) = \mu_{\rm nc}(T,V) G\left[\frac{\mu_{\rm nc}(T,V)H}{k_{\rm B}T}\right], \qquad (16)$$

with the function $G(x)$ defined by:

$$G(x) = \frac{1}{2}\int_0^{\pi} {\rm d}\theta \sin\theta\cos\theta\tanh(x\cos\theta). \qquad (17)$$

The $G(x)$ function is plotted in the inset of Figure 10 together with the Langevin function $L(x)$; $G(x)$ saturates at the value 1/2, whereas the Langevin law saturates at unity. The isothermal magnetization curves have been fitted with this model of dynamic "random magnetic orientation", according to the law:

$$M(T,H) = \chi_{\rm AF}(T)H + \frac{1}{\langle V\rangle}\int_{V_{\rm min}}^{V_{\rm max}} \mu_{\rm nc}(T,V) f(V) G\left[\frac{\mu_{\rm nc}(T,V)H}{k_{\rm B}T}\right] {\rm d}V, \qquad (18)$$

where $f(V)$ is the lognormal volume distribution function. We chose to describe the uncompensated moments by their mean value: $\mu_{\rm nc}(T,V) = m_0 u(T)\sqrt{N}$, where $u(T)$ accounts for the thermal variation of a Fe^{3+} moment. In Figure 10 are represented the low field parts of the isothermal magnetization curves in the particles with 982 Fe atoms per core, at 35 K and 80 K, together with the fits of the data using the $G(x)$ function (solid line) and the Langevin function (dashed line) with the same volume distribution. It is clear that the fit using the "random magnetic orientation" model gives a better account of the $M(H)$ curvature at low fields than does the Langevin fit, the improvement being more pronounced at low temperature. The complete field and temperature variation of the magnetization in the particles with 982 Fe atoms per core is shown in Figure 11, the solid lines representing the fit using the "random magnetic orientation" model (Eq. (18)).

These fits are very satisfactory in the whole field range, and the values for u are about 0.6 (close to those obtained in the Mössbauer spectra at 90 K at the lowest fields) and slowly decrease as temperature increases. We emphasize that the description of the thermal and field variation of the uncompensated magnetization in the superparamagnetic regime using the $G(x)$ function lies on stronger physical grounds than that using a Langevin function. The upper bound of the field range where this approach is valid, as discussed in Section 6, is approximately $H_{\rm A}/\alpha$, *i.e.* it is close to the maximum field (5–6 T) used so far in magnetization studies of ferritin. Above this field, the uncompensated magnetization starts to decrease and vanishes when the field reaches the spin-flop threshold, as the uncompensated moments fluctuate along a direction close to perpendicular to the applied field. The $G(x)$ function has been evoked by Néel [16,25] in his studies of antiferromagnetic particles: he applied it to calculate the thermoremanent magnetization at the blocking temperature and stated that it was the correct description of the uncompensated magnetization in the limit of strong anisotropy. This fact has also been noted by Bean [29] for the magnetization of ferromagnetic fine powders. We showed here that, in weakly uncompensated antiferromagnetic particles (*i.e.* with a degree of uncompensation of a few percent), the $G(x)$ function yields a correct description of the magnetization even for finite and rather small values of the anisotropy energy, like those found in ferric oxides, for fields up to 5–6 T. This is finally a consequence of the very large value of the exchange field, which yields a large spin-flop field.

The thermal variation of the mean uncompensated moment derived from our fits of the $M(H)$ curves presents a small but significant decrease as temperature increases from 35 K to 250 K, for all particle sizes. Using an antiferromagnetic magnon law: $\mu_{\rm nc}(T) = \mu_{\rm nc}(0)(1-\alpha T^2)$, the experimental $\mu_{\rm nc}(T)$ curves can be extrapolated to zero in order to yield an estimation of the Néel temperature. We find that $T_{\rm N}$ is close to 500 K, and that it is practically the same for all particle sets. This absence of dependence of $T_{\rm N}$ on the mean particle size is probably due to the fact that the distance between "active" reticular planes, which determines the strength of the superexchange interaction, is independent of the particle size. The $T_{\rm N}$ value we obtain is roughly two times larger than early estimations [3,4], but is in good agreement with more recent determinations [5,9,10] in natural ferritin.

The antiferromagnetic susceptibility $\chi_{\rm AF}(T)$, shown in the inset of Figure 11 for the particles with 982 Fe atoms per core, decreases with increasing temperature, whereas the bulk powder antiferromagnetic susceptibility is expected to increase on heating. A mechanism for the thermal decrease of $\chi_{\rm AF}$ has been proposed by Néel [25], by considering the reduced exchange field of the superficial Fe layers, but it is difficult to say whether it is responsible for the thermal decrease of $\chi_{\rm AF}$ we observe in the ferritin particles. The $T = 0$ value of $\chi_{\rm AF}$, derived from the magnetization curves at 2.5 K (not shown here), amounts to a few 10^{-4} emu/cm^3 for all particle sets. In the simple molecular field model, the expression for the powder T=0 antiferromagnetic susceptibility is: $\chi_{\rm AF}(T=0) = \frac{2}{3}\chi_{\perp} = \frac{2}{3}(M_0/H_{\rm E})$. Using the estimated exchange field value $H_{\rm E} = 320$ T, we find that, for each particle set, the calculated $\chi_{\rm AF}(T=0)$ is smaller than

the experimental value by a factor of about 3. Néel showed that the susceptibility of antiferromagnetic particles having an even number of "active" reticular planes (*i.e.* no net magnetic moment) can be enhanced by a factor 2 or more with respect to the bulk susceptibility, and that this is a surface effect visible in very small particles [30]. He called this behaviour "superantiferromagnetism". We think that this mechanism is effective for such particles even in the presence of a small uncompensated moment, and that it is responsible for the observed large value of the antiferromagnetic susceptibility. The superantiferromagnetic behaviour is confirmed by high field (30 T) magnetization measurements we performed at 2.5 K in natural ferritin, which will be the subject of a future publication [31].

At this stage, we would like to comment on the observability of effects linked with surface atoms in antiferromagnetic particles. Due to the small size of our particles (4–6 nm), an important fraction of Fe atoms (around 40%) lie at the surface, and their properties (anisotropy, exchange field) are likely to be somehow different from those of the core atoms. For instance, in ferro- or ferrimagnetic systems, the observed lack of full alignment of the magnetic moments with the applied field is characteristic of nanoparticles and is generally attributed to the different behaviour of surface atoms [18,32]. In antiferromagnetic particles in moderate magnetic fields, the situation is different because the dominant configuration is an almost random orientation of the moments with respect to the field. Then, effects linked with surface moments are much more difficult to evidence experimentally and to distinguish from those due to core moments (see however Ref. [33]). So, although the properties of surface atoms may be different from those of the core atoms in our artificial ferritin particles, we could not detect their effects in our experimental data, except for the superantiferromagnetic behaviour mentioned above.

8 Conclusion

We performed ^{57}Fe Mössbauer absorption spectroscopy and magnetization measurements in antiferromagnetic artificial ferritin particles, with mean Fe loadings ranging from 400 to 2 500 atoms, in the temperature range 2.5–250 K and with magnetic fields up to 7 T. In zero or very low field, the dynamics of the sublattice magnetization of the ferritin particles obeys classical superparamagnetic relaxation in the thermal activation regime. The value of the anisotropy energy per unit volume K could be determined from the FC-ZFC susceptibility curves and from the thermal variation of the Mössbauer superparamagnetic fraction. The values obtained by both techniques are in good agreement and are in the range $3\text{–}6 \times 10^5$ ergs/cm^3, typical for ferric oxides or hydroxides, with a tendency for K to increase as the particle size decreases. By comparing the data obtained by Mössbauer spectroscopy and by magnetometry in moderate magnetic fields up to 7 T, we propose a new interpretation of the field and temperature behaviour of the uncompensated magnetization in the superparamagnetic regime. We show that it is better described by a "random magnetic orientation" model, where the uncompensated moments fluctuate along the antiferromagnetic axis, than by the usually assumed Langevin law. This behaviour is described by the universal function:

$$G(x) = \frac{1}{2}\int_0^\pi \mathrm{d}\theta\, \sin\theta\cos\theta\tanh(x\cos\theta). \qquad (19)$$

To our knowledge, this law has never been applied to the interpretation of data in antiferromagnetic particles, although Néel had noticed that it should be the correct description of the thermal and field variation of the uncompensated magnetization in the limit of large anisotropy [25]. We think this non-Langevin behaviour actually holds for usual values of the anisotropy energy, and it should be valid not only in ferritin, but also in other weakly uncompensated antiferromagnetic particles, at least in moderate magnetic fields. As the field is increased towards the spin-flop field (10–20 T) and above, the "random magnetic orientation" picture breaks down, as the magnetic moments progressively reorient perpendicular to the applied field and the superparamagnetic uncompensated magnetization vanishes.

We could also estimate the Néel temperature in our artificial ferritin samples by following the decrease of the mean uncompensated moment in the temperature range 35–250 K; we find that T_N is essentially independent of the mean particle size, and that it is close to 500 K, in agreement with other recent estimations.

The authors are grateful to Dr E. Vincent and Dr G. LeBras, from the Service de Physique de l'État Condensé (CEA Saclay), for their help with the SQUID measurements.

References

1. T.G. St. Pierre, J. Webb, S. Mann, in *Biomineralization: Chemical and Biochemical Perspectives*, edited by S. Mann, J. Webb, R.J.P. Williams (VCH, New-York, 1989), Chap. 10.
2. F.C. Meldrum, V.J. Wade, D.L. Nimmo, B.R. Heywood, S. Mann, Nature **349**, 684 (1991).
3. S.H. Bell, M.P. Weir, D.P.E. Dickson, J.F. Gibson, G.A. Sharp, T.J. Peters, Biochim. Biophys. Acta **787**, 227 (1984).
4. E.P. Bauminger, I. Nowik, Hyperfine Interact. **50**, 489 (1989).
5. T.G. St. Pierre, D.H. Jones, D.P.E. Dickson, J. Magn. Magn. Mat. **69**, 276 (1987).
6. Q.A. Pankurst, R.J. Pollard, J. Phys. Cond. Mat. **2**, 7329 (1990).
7. C. Hunt, Q.A. Pankhurst, D.P.E. Dickson, Hyperfine Interact. **91**, 821 (1994).
8. S.H. Kilcoyne, R. Cywinsky, J. Magn. Magn. Mat. **140**, 1466 (1995).
9. S.A. Makhlouf, F.T. Parker, A.E. Berkowitz, Phys. Rev. B **55**, R14 717 (1997).

10. R.A. Brooks, J. Vymazal, R.B. Goldfarb, J.W.M. Bulte, P. Aisen, Magn. Reson. Med. **40**, 227 (1998).
11. J.G.E. Harris, J.E. Grimaldi, D.D. Awschalom, A. Chiolero, D. Loss, Phys. Rev. B **60**, 3453 (1999).
12. B. Barbara, E.M. Chudnovsky, Phys. Lett. A **145**, 205 (1990).
13. D.D. Awschalom, J.F. Smyth, G. Grinstein, D.P. DiVincenzo, D. Loss, Phys. Rev. Lett. **68**, 3092 (1992).
14. S. Gider, D.D. Awschalom, T. Douglas, S. Mann, M. Chaparala, Science **268**, 77 (1995).
15. J. Tejada, X.X. Zhang, E. del Barco, J.M. Hernandez, E.M. Chudnovsky, Phys. Rev. Lett. **79**, 1754 (1997).
16. L. Néel, J. Phys. Soc. Jpn **17**, Supp. B 1, 676 (1962).
17. L. Néel, C. R. Acad. Sciences, Paris **252**, 4075 (1961).
18. R.H. Kodama, A.E. Berkowitz, E.J. McNiff Jr., S. Foner, Phys. Rev. Lett. **77**, 394 (1996).
19. L. Néel, Ann. Geophys. **5**, 99 (1949).
20. W. F. Brown Jr., Phys. Rev. **130**, 1677 (1963).
21. L. Néel, C. R. Acad. Sciences, Paris **253**, 9 (1961).
22. J.I. Gittleman, B. Abeles, S. Bozowski, Phys. Rev. B **9**, 3891 (1974).
23. S. Bocquet, R.J. Pollard, J.D. Cashion, J. Appl. Phys. **77**, 2809 (1995).
24. R. Sappey, E. Vincent, N. Hadacek, F. Chaput, J.P. Boilot, D. Zins, Phys. Rev. B **56**, 14551 (1997).
25. L. Néel, in *Physique des basses températures*, edited by C. DeWitt, B. Dreyfus, P.G. De Gennes (Gordon and Breach, New York, 1962).
26. V. Beckmann, W. Bruckner, W. Fuchs, G. Ritter, H. Wegener, Phys. Status Solidi **29**, 781 (1968).
27. S. Mørup, Surf. Sci. **156**, 888 (1985).
28. M. Hanson, C. Johansson, S. Mørup, J. Phys. Cond. Mat. **5**, 725 (1993).
29. C.P. Bean, J. Appl. Phys. **26**, 1381 (1955).
30. L. Néel, C. R. Acad. Sciences, Paris **253**, 203 (1961); **253**, 1286 (1961).
31. C. Gilles, P. Bonville, H. Rakoto, J.M. Broto, K.K.W. Wong, S. Mann (to be published).
32. A.H. Morrish, K. Haneda, J. Magn. Magn. Mat. **35**, 105 (1983).
33. R.H. Kodama, S.A. Makhlouf, A.E. Berkowitz, Phys. Rev. Lett. **79**, 1393 (1997).